J MATER SCI **41** (2006) 2553–2557

Atomic structure of AlN/Al_2O_3 interfaces fabricated by pulsed-laser deposition

Y. TOKUMOTO*, Y. SATO, T. YAMAMOTO
Department of Advanced Materials Science, Graduate School of Frontier Science, The University of Tokyo, Kashiwa, Chiba, Japan
E-mail: tokumoto@sigma.t.u-tokyo.ac.jp

N. SHIBATA, Y. IKUHARA
Institute of Engineering Innovation, School of Engineering, The University of Tokyo, Bunkyo-ku, Tokyo, Japan

Published online: 17 April 2006

The atomic structure of AlN/Al_2O_3 interface fabricated by pulsed laser deposition is characterized by high-resolution transmission electron microscopy (HRTEM) combined with systematic multi-slice HRTEM image simulations. It is found that the AlN film deposited on a (0001) Al_2O_3 substrate grows epitaxially with the orientation relationship of (0001)AlN//(0001) Al_2O_3 and $[\bar{1}100]AlN//[11\bar{2}0]Al_2O_3$, with an atomically sharp interface. The observed interface showed best correspondence with the rigid structural model that AlN is terminated by Al at the interface, while the Al_2O_3 substrate is terminated by O. Detailed structural analysis indicates that Al sites at the interface are coordinated by both oxygen and nitrogen in this model, with similar coordination environment in AlN. This favored coordination state at the interface may stabilize the AlN/Al_2O_3 interface.

1. Introduction

The growth of defect-free or low-defect films has been a key issue for the thin-film optoelectronic/microelectronic technology. GaN film is one of the most widely applied film systems because of its wide and tunable energy band gaps suitable for optoelectronic device applications [1–3]. Since residual defects in the film are known to degrade its properties, extensive studies to reduce the internal defects have been performed [4, 5]. The misfit between GaN and the Al_2O_3 substrate has been noticed as the source of many types of defects in the film [6, 7]. It is demonstrated that an AlN buffer layer can effectively reduce the misfit, and assist the growth of high-quality GaN films [4]. This indicates that the effective relaxation of lattice mismatch at the interface is critical for the film quality. However, residual defects in the AlN layer also inevitably promote the formation of defects in GaN films. Thus, the relaxation and defect formation mechanism at the AlN/Al_2O_3 interface must be clarified in order to control the film quality, and hence device property of the GaN film on an AlN buffer layer. Although there are a few reports regarding the AlN/Al_2O_3 interface [8, 9], its detailed atomic structure has not been clarified. Here, we characterize the atomic structure of the AlN/Al_2O_3 interface fabricated by pulsed-laser deposition (PLD), using high-resolution transmission electron microscopy (HRTEM) in conjunction with systematic multi-slice image simulations. Favored crystal orientation and interface structure were characterized, and the formation mechanism of the AlN/Al_2O_3 interface at an atomistic scale is discussed.

2. Experimental procedure

AlN thin films were grown on (0001) α-Al_2O_3 substrates by PLD. A KrF excimer laser beam (wavelength, 248 nm; repetition frequency, 10 Hz) was focused onto an AlN ceramic target to produce an energy density of 0.5 J/cm^2·pulse. The deposition was made of a substrate temperature of 750°C and a backpressure of 7×10^{-5} Pa.

Cross-sectional TEM thin foils were prepared by conventional methods including mechanical polishing and argon-ion-beam thinning to obtain an electron transparency. Conventional and high-resolution TEM

*Author to whom all correspondence should be addressed.
0022-2461
DOI: 10.1007/s10853-006-7767-1

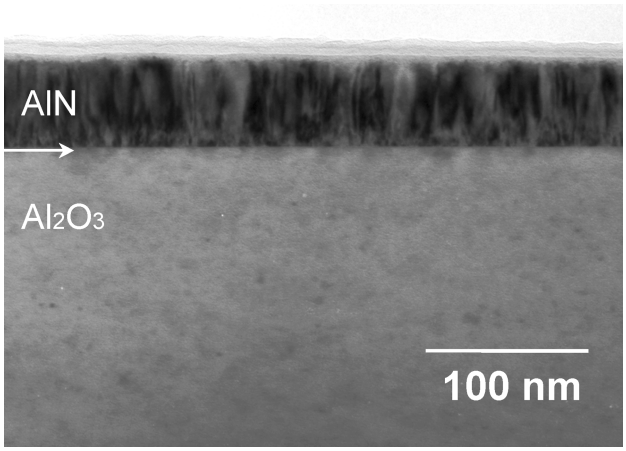

Figure 1 Cross-sectional TEM bright-field image of the AlN film deposited on the Al_2O_3 substrate. An arrow shows the position of the interface. No secondary phase was observed at the interface. Weak contrast observed on the upper side of the AlN surface is an amorphous layer, which is formed during argon-ion-beam thinning. Linear contrast vertical to the interface indicates residual strain and/or defects inside the film.

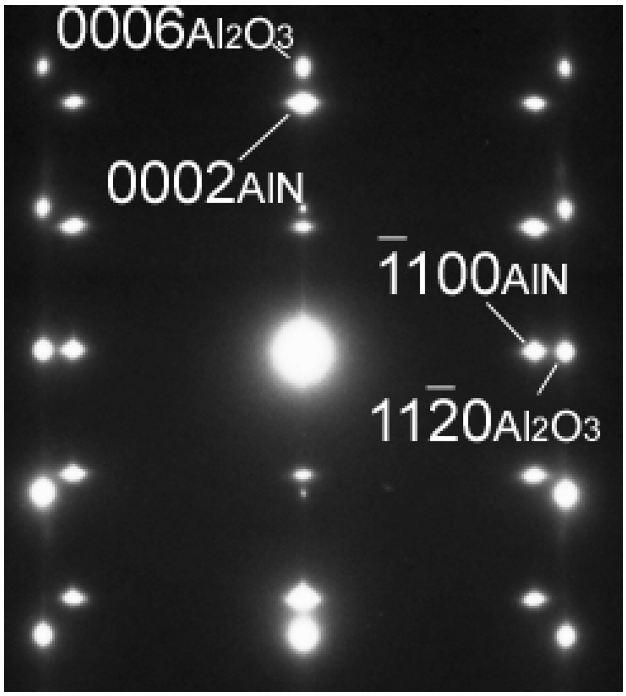

Figure 2 Selected-area diffraction pattern taken from the interface region. AlN clearly shows a single-crystal pattern, although the spots seem to be a little bit elongated, which also indicates the strain and/or defects inside the film. The predominant orientation relationships of $(0001)AlN//(0001)Al_2O_3$ and $[\bar{1}100]AlN//[11\bar{2}0]Al_2O_3$ is found in the pattern.

observations were made using JEM-2010HC and JEM-4010 microscopes (JEOL Co. Ltd), operated at 200 kv and 400 kV, respectively.

To investigate the atomic structure of the AlN/Al_2O_3 interface, HRTEM image simulations with the Tempas program code [10] based on the multi-slice method [11] were conducted. HRTEM images were systematically simulated as a function of defocus and sample thickness to yield an appropriate match to experimental images.

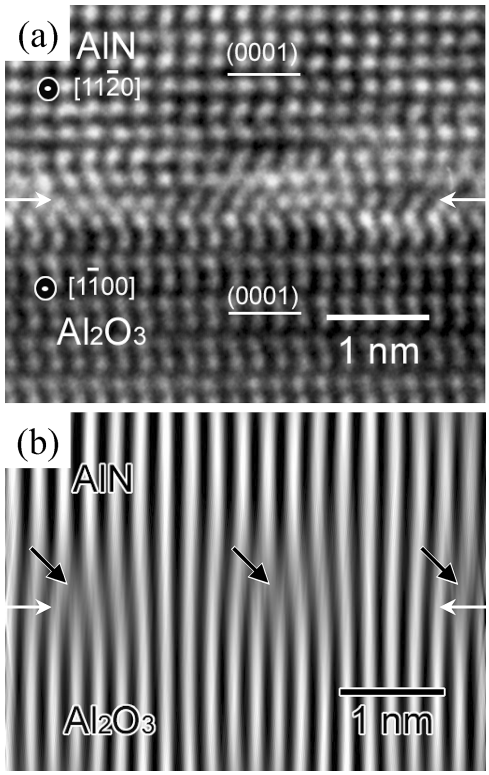

Figure 3 (a) HRTEM image of the interface. The incident beam direction is parallel to $[11\bar{2}0]$ and $[1\bar{1}00]$ in AlN and Al_2O_3, respectively. (b) Fourier filtered image obtained from the above experimental image. Frequency components of $(\bar{1}100)$ in AlN and $(11\bar{2}0)$ and in Al_2O_3 are respectively enhanced to visualize lattice misfits at the interface. Obvious lattice misfits are observed at the interface.

3. Results and discussion

Fig. 1 shows a cross-sectional TEM image of the AlN film deposited on the Al_2O_3 substrate. The thickness of the AlN film is measured to be about 50 nm. Vertical contrast seen in the AlN film indicates residual strain and/or defects. No secondary phase is observed at the film/substrate interface. A diffraction pattern from the interface region is shown in Fig. 2. It is clearly seen that deposited AlN shows a single-crystal pattern, having a preferential orientation relationship with the Al_2O_3 substrate. The predominant orientation relationship between the AlN film and Al_2O_3 substrate is determined to be $(0001)AlN//(0001)Al_2O_3$ and $[\bar{1}100]AlN//[11\bar{2}0]Al_2O_3$ from the pattern. The present orientation relationship is consistent with the previously reported AlN/Al_2O_3 interface fabricated by a different deposition technique (molecular beam epitaxy (MBE)) [8]. According to the geometrical coherency estimated by the coincidence of reciprocal lattice points (CRLP) method [12], the present orientation is one of the highly coherent ones between AlN and α-Al_2O_3 crystal structures [13].

Fig. 3a shows a HRTEM image of the AlN/Al_2O_3 interface. The image was taken along the [$1\bar{1}00$] direction of the Al_2O_3 substrate. The arrow indicates the position of the interface, which is seen to be atomically sharp without any intermediate secondary phases even on an atomistic scale. Fig. 3(b) shows a filtered image of Fig. 3a, enhancing the frequency components perpendicular to the interface. As shown by the black arrows, lattice misfit was periodically introduced in every 8 atomic planes of AlN (9 atomic planes of Al_2O_3). This is also consistent with the previous report by Kehagias *et al*. by MBE [8].

The misfit parameter δ, between AlN and Al_2O_3 can be estimated by the following formula by taking AlN as the reference crystal,

$$\delta_{\mathrm{AlN}[\bar{1}100]/\mathrm{Al_2O_3}[11\bar{2}0]} = \frac{d_{(\bar{1}100)\mathrm{AlN}} - d_{(11\bar{2}0)\mathrm{Al_2O_3}}}{d_{(\bar{1}100)\mathrm{AlN}}} = \frac{\sqrt{3\alpha}_{\mathrm{AlN}} - \alpha_{\mathrm{Al_2O_3}}}{\sqrt{3\alpha}_{\mathrm{AlN}}} \quad (1)$$

where d and a correspond to the interplanar spacing and lattice parameter of each crystal ($a_{\mathrm{AlN}} = 0.308$ nm, $a_{\mathrm{Al_2O_3}} = 0.4763$ nm), respectively [14 , 15]. The misfit parameter obtained is about 11%, which is categorized as a large lattice-mismatched system [16]. The periodic misfits as shown in Fig. 3(b) must be geometrically introduced to accommodate the large lattice misfits between AlN and Al_2O_3.

In order to determine the atomic structure of the interface, possible structural models were constructed by using rigid AlN and Al_2O_3 crystal structures. On constructing the structural models, the direction of the lattice polarity of AlN layers, in addition to the termination of the Al_2O_3 substrate, was taken into account separately. Here, we neglected the oxygen-nitrogen bonded interface models, which showed completely different interface images by our preliminary image simulations. Four possible structural models can be constructed for the present interface. Fig. 4 shows the four possible structural models (top) and the corresponding simulated HRTEM images (bottom). We define models in Fig. 4a–d as models (**A**–**D**), respectively. In terms of the lattice polarity of the AlN film, the four structural models are divided into two groups. In models **A** and **B**, the film has the *N*-polarity, while models **C** and **D** have Al-polarity. The termination of the Al_2O_3 substrate is different in each group; models **A** and **C** are terminated by oxygen planes, while models **B** and **D** are terminated by aluminum planes. Since the ionic radii of anions in AlN and Al_2O_3 are rather larger than that of cations ([17]), we built structural models based on the anion sublattice [18]. Therefore, interlayer distances were determined to maintain N–O bond distances as about 0.285 nm, which is intermediate value between N–N (0.307 nm) in AlN and O–O in Al_2O_3 (0.263 nm). Image simulations were performed over a range of thicknesses and defocus values, systematically. The simulated HRTEM images shown in Fig. 4e–h were obtained for a crystal thickness of 5 nm and a defocus value of –38 nm which is close to Scherzer defocus of the present microscope (about –41 nm).

Through systematic comparison between the experimental and simulated HRTEM images in the interface region, models **A** and **D** can be chosen as candidates for the interface structure, even though the strain effect is

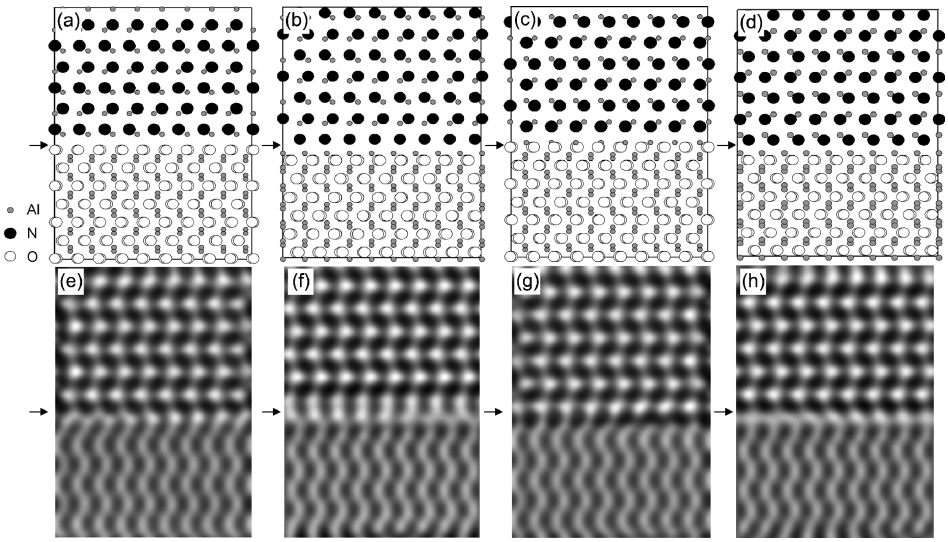

Figure 4 (a–d) Structural models constructed from AlN (upper) and Al_2O_3 (lower) half-crystals. Al, N, and O atoms are denoted as gray, black, and white circles, respectively. The orientation relationship of the models is the same as observed, that is, (0001)AlN//(0001)Al_2O_3 and [$\bar{1}$100]AlN//[$11\bar{2}0$]Al_2O_3. As noted in the text, the four models differ in termination layers of both half-crystals and the lattice polarity in AlN. (e–h) Simulated HRTEM images obtained from the models in (a–d). The simulations were conducted for a specimen thickness of 5 nm and defocus of –38 nm.

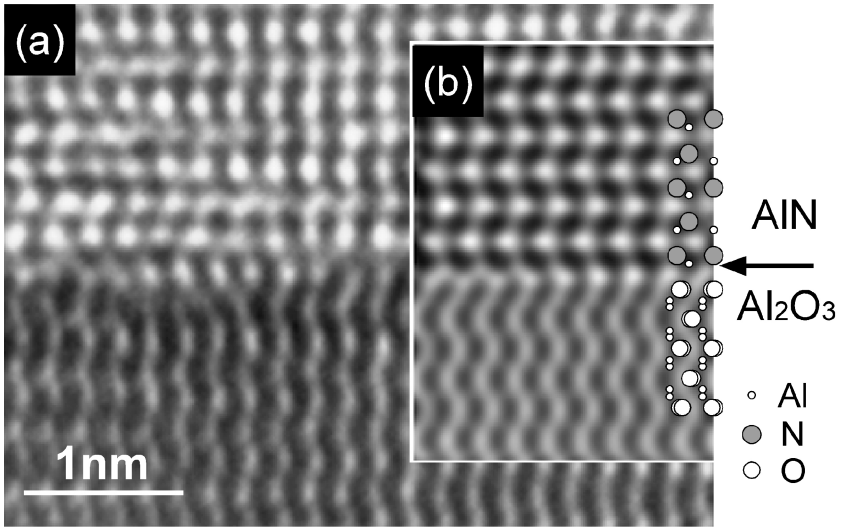

Figure 5 Comparison between (a) experimental and (b) simulated HRTEM images. The simulated image in Fig. 4e, which is based on model **A** in Fig. 4 a, is embedded in the experimental one. Respective atomic positions are superimposed in (b).

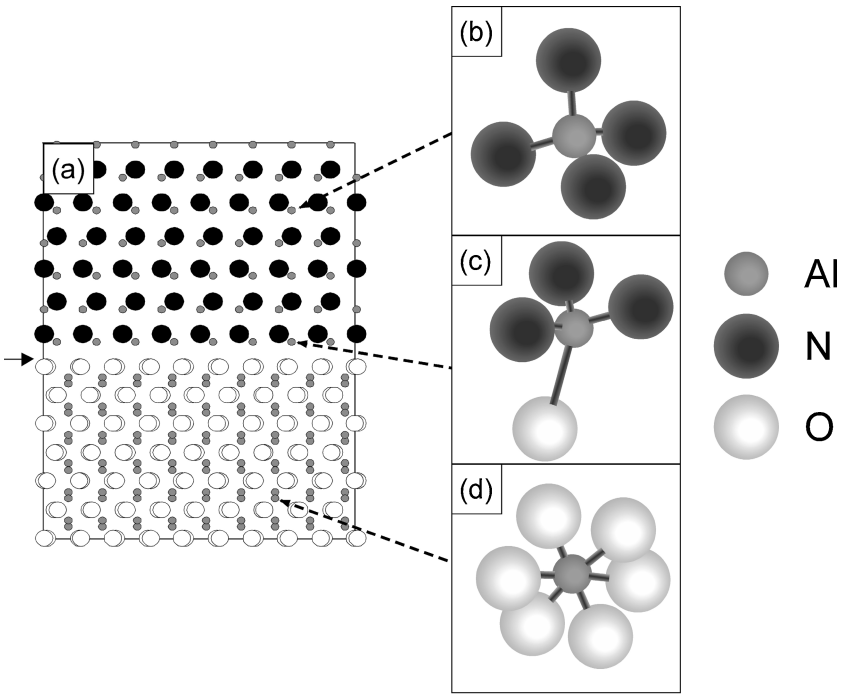

Figure 6 Schematic of Al^{3+} coordination through the interface. The structural model A is again displayed in (a). Al^{3+} coordination in AlN crystal, at the interface, and in Al_2O_3 crystal is illustrated in (b–d), respectively.

not taken into account in the present models. Comparing the two images obtained from models **A** and **D**, the bright intensity at the very interface is more continuous and elongated parallel to the interface in model **D** than **A**. From this point, the experimental image can be considered to fit better model **A**. As demonstrated in Fig. 5, the superimposed simulated image of model **A** agrees well with the experimental HRTEM image. This suggests that model **A** is the most likely model for the present AlN/Al_2O_3 interface structure.

Here, a question arises as to why model **A** is experimentally preferred over model **C** with the same crystal termination but different polarity. This indicates that the interface structure may affect the growth direction of the AlN film on an Al_2O_3 substrate. As we compare models **A** and **C** in detail, the interface Al atomic sites take completely different coordination environment in the two models. Fig. 6 shows schematic illustrations of Al coordination polyhedra across the AlN/Al_2O_3 interface. Al takes 4-fold coordination of *N* in AlN, while it takes

6-fold coordination of O in Al_2O_3. At the very interface, Al are coordinated by both O and N, and mostly take 4-fold coordination ($3 \times$ N and $1 \times$ O as in Fig. 6c) along the interface. According to Pauling's empirical law of the relative stability of crystal structures in ionic crystals [19], cations prefer higher coordination environment by anions as possible. In model **A**, Al ions can preserve high coordination number of anions even at the very interface, and coordination number changes from 4 (AlN), 4 (interface) and 6(Al_2O_3) across the interface. On the other hand, Al sites along the interface are ought to take 3-fold coordination in model **C** because of the different lattice polarity to model A. This indicates that the Al at the interface would be highly miscoordinated, which might cause higher interfacial energy, and hence become less stable than the interface structure in model **A**. Thus, the interface structure of model **A** should be energetically favorable even if the crystal termination of the Al_2O_3 substrate is identical.

It is suggested that the crystal polarity of the AlN film on Al_2O_3 strongly depends on the deposition condition, such as Al- or N-rich condition [20]. Although further work is needed in order to confirm the predicted crystal polarity of the present film, the result suggests that the crystal polarity is related to the interface atomic structure. A difference in deposition condition may enhance the formation of different interface structures, and as a result, the crystal polarity of growing film varies.

4. Summary

The atomic structure of the AlN/Al_2O_3 interface fabricated by PLD is investigated by HRTEM combined with systematic multi-slice HRTEM image simulations. It is found that the AlN film deposited on a (0001) Al_2O_3 substrate has the orientation relationship of (0001)AlN//(0001)Al_2O_3 and $[\bar{1}100]$AlN//$[11\bar{2}0]Al_2O_3$, with an atomically sharp interface. The observed interface showed best correspondence with the structure model in which AlN is terminated by an Al layer at the interface, while the Al_2O_3 substrate is terminated by an O layer. The model structure suggests that the Al sites at the interface are coordinated by both O and N. This favored coordination at the interface may be the reason why the present interface structure is stable.

Acknowledgments

This study was financially supported by a Grant-in-Aid for Scientific Research and Special Coordination Funds from the Ministry of Education, Culture, Sports, Science and Technology, and Japan Society of Promotion of Science, (JSPS) Japan. One of the authors (YS) is supported as a JSPS research fellow.

Reference

1. S. NAKAMURA, M. SENOH and T. MUKAI, *Jpn. J. Appl. Phys.* **32** (1993) L8.
2. S. NAKAMURA, M. SENOH, S. NAGAHAMA, N. IWASA, T. YAMADA, T. MATSUSHITA, H. KIYOKU and Y. SUGIMOTO, *ibid.* **35** (1996) L74.
3. H. AMANO, T. ASAHI and I. AKASAKI, *ibid.* Part 2, 29 (1990) L205.
4. S. YOSHIDA, S. MISAWA and S. GONDA, *Appl. Phys. Lett.* **42** (1983) 427.
5. S. C. JAIN, M. WILLANDER, J. NARAYAN and R. VAN OVERSTRAETEN, *J. Appl. Phys.* **87** (2000) 965.
6. S. D. LESTER, F. A. PONCE, M. G. CRAFORD and D. A. STEIGERWALD, *Appl. Phys. Lett.* **66** (1995) 1249.
7. P. RUTERANA, V. POTIN, B. BARBARAY and G. NOUET, *Phil. Mag.* **A80** (2000) 937.
8. Th. KEHAGIAS, Ph. KOMNINOU, G. NOUET, P. RUTERANA and Th. KARAKOSTAS, *Phys. Rev.* **B64** (2001) 195329.
9. J. R. HEFFELFINGER, D. L. MEDLIN and K. F. MCCARTY, *J. Appl. Phys.* **85** (1999) 466.
10. R. KILAAS, Proc., of the 49th Electron Microscopy Society of America Meeting, edited by G. W. Bailey (San Francisco Press, 1991) p. 258.
11. J. M. COWLEY and A. F. MOODIE, *Acta Crystallogr.* **10** (1957) 609.
12. Y. IKUHARA and P. PIROUZ, *Mater. Sci. Forum.* Part I **207–209**, (1996) 121.
13. T. SASAKI, private communication.
14. K. M. TAYLOR and C. LENIE, *J. Electrochem. Soc.* **107** (1960) 308.
15. L. PAULING and S. B. HENDRICKS, *Phys. Rev.* **122** (1925) 757.
16. Y. IKUHARA and P. PIROUZ, *Micros. Res. Techn.* **40** (1998) 206.
17. R. D. SHANNON, *Acta Crystallogr.* **A32** (1976) 751.
18. P. KUNG, C. J. SUN, A. SAXLER, H. OHSATO and M. RAZEGHI, *J. Appl. Phys.* **75** (1994) 4515.
19. W. D. KINGERY, H. K. BOWEN and D. R. UHLMANN, "Introduction to Ceramics", 2nd ed. (John Wiley & Sons, New York, 1976).
20. Q. S. PADUANO, D. W. WEYBURNE, J. JASINSKI and Z. LILIENTAL-WEBER, *J. Crystal Growth*, **261** (2004) 259.